CU Journal of Non-Linear Fluid Mechanics
Vol. 02, No. 01, 2026
https://doi.org/10.11615/cujnlfm.02101-2

A Computational Study on the Radiative Thermal Transport of Nanofluids Past a Stretching Boundary

Hanafi A Rahim*[a]

[a] Faculty of Computer Science and Mathematics, Universiti Malaysia Terengganu, Terengganu, Malaysia

Abstract

The present study deals with the thermal analysis of a nanofluid past the stretching sheet in presence of radiation. Thermal and mass transport are also modelled considering viscous dissipation and the effects of chemical reaction. Additionally, temperature-dependent and concentration-dependent heat source terms are incorporated into the energy equation to examine their influence on the thermal transport characteristics of the nanofluid. An increase in the internal heat generation parameter enhances the temperature distribution within the boundary layer due to the additional volumetric heat supplied to the fluid, thereby thickening the thermal boundary layer and reducing the wall temperature gradient. Thus, this is incorporated into the energy equation. The governing equations were formulated using partial differential equations (PDEs). These equations are then transformed into ODEs through the application of similarity transformations to obtain the solution. The resulting system of ODEs is subsequently solved using the Runge–Kutta–Fehlberg (RKF45) method. The effect of the dimensionless parameters on the nanofluid's temperature, concentration, and velocity profiles is presented graphically using the numerical solutions. The outcomes of the study depicts that the temperature profile upsurges when the heat source dependent on temperature and the concentration increases. It was noted that there is a lowering in the velocity profile with rise in the velocity slip parameter while the thermal profile increases with increase in thermal radiation.

Keywords: Magnetic field; temperature dependent heat source; concentration dependent heat source; chemical reaction rate; nanofluid.

1 Introduction

The behaviour of an electrically conductive fluids under the influence of magnetic fields, such as plasmas, liquid metals, or seawater, is studied by magnetohydrodynamics (MHD). It combines concepts from electromagnetic and fluid dynamics to explain how fluid flow is influenced by magnetic fields and vice versa. In fields like fusion research, astrophysics, and engineering systems like liquid metal cooling, MHD is an essential element. Patel and Patel [1] found that magnetic parameter reduces the temperature profile of fluid. Jamrus et al. [2] found that the rise in the magnetic parameter lowers the rate of heat transmission. Hajool and Harfash [3] found that the stability of the system increases as permeability ratio increases. Magnetic and

* hanafi@umt.edu.my

suction parameters increase the thermal profile as shown by Waini et al. [4]. Fard et al. [5] discovered that increasing the heat transfer efficiency reduces the energy loss.

The term viscous dissipation describes the process by which internal friction, or viscous friction, transforms mechanical energy into internal energy. This effect can affect the fluid system's thermal behaviour and is substantial in flows with high viscosities or velocities. It is a crucial factor to take into account in fluid dynamics and heat transfer. Rehman and Khan [6] analysed the impact of nanofluid parameters on the velocity and thermal distribution in mixed convective flow of hybrid nanofluids. Rehman et al. [7] found that the increase in the couple-stress parameter reduces the velocity profile. Haq and Ashraf [8] found that the temperature profile rises with nonlinear radiation parameter. Awais et al. [9] studied velocity profile variations with Hartman number for a MHD Eyring-Powell fluid flow. Maaitah et al. [10] analysed velocity profile behaviour with increase in Darcy number. Zhang et al. [11] studied the effect of oil viscosity and analysed that temperature characteristics enhanced after luminescence. Rudyak [12] analysed the behaviour of nanofluid flows and reported that nanofluids facilitate attaining substantially higher heat transfer coefficients. Nuriev et al. [13] studied on cylindrical bodies and flows induced due to oscillations.

When there is a temperature gradient inside a body, heat transfer occurs, and when there is a concentration gradient, mass transfer happens. Heat and mass transfer are essential to many processes, including those in the natural world and in industrial settings. Heat transfer, which drives processes like power generation, cooling, and heating, controls the exchange of thermal energy, whereas mass transfer is crucial for procedures like chemical reactions, drying, and distillation. These processes affect product development, environmental effects, and energy efficiency. Majeed et al. [14] observed that drag and lift coefficients decrease with the magnetic parameter. Abbas et al. [15] found that velocity profile varies increasingly with a rise in the fractional parameter. Ahmad et al. [16] discovered that heat and mass transfer increases as the Rayleigh number grows. Karim et al. [17] analysed temperature, concentration fields, and patterns of fluid flow are all impacted by a moving wall in a right triangular cavity. Kumar et al. [18] found that as chemical reaction increases, velocity profile rises. Menni et al. [19] analysed the enhancement of heat transfer performance and found that perforated obstacles have the potential to significantly improve the efficiency of heat exchangers.

The Thompson and Troian slip model, particularly in relation to nanofluidic and microfluidic systems, describes the fluid flow near a solid boundary when there is a partial slip. When there is slip at the boundary, a non-zero velocity of fluid is allowed; a zero-velocity condition at the boundary is known as a no-slip condition. Slip models serve as a vital tool for understanding fluid behaviour at the nanoscale, where traditional no-slip boundary criteria might not hold true. One such slip model was introduced by Thompson and Troian [20] at the solid surface where a general nonlinear relation exists between the slip and local shear rate. Xin et al. [21] found that heat conduction increases with increase in thermophoresis parameter. Shaheen et al. [22] found that the thermal field is enhanced with an upsurge in the conjugate parameter for Newtonian heating. Mishra et al. [23] discovered that the Nusselt number increases with higher velocity slip parameter. Chaudhary and Deshwal [24] found that thermal profile decreases with increase in Soret number.

When disseminated throughout a fluid, nanoparticles enhance the base fluid's ability to transfer heat and produce additional effects. Its capacity to produce heat is one of the important effects. In systems like heat exchangers and microchannel flows, where different nanoparticle concentrations can improve thermal conductivity and efficiency, concentration-dependent heat sources are employed to promote heat transfer. Although numerous studies have investigated MHD nanofluid flow, thermal radiation, viscous dissipation, chemical reactions, and slip effects, relatively limited attention has been given to the combined influence of temperature-dependent and concentration-dependent heat sources on the coupled heat and mass transfer characteristics of a radiative nanofluid over a stretching sheet. In addition, the incorporation of the nonlinear Thompson–Troian slip condition together with an externally applied magnetic field provides an important extension of the existing formulation.

In addition, the surface is exposed to the Troian and Thompson slip conditions when a magnetic field is present. The governing differential equations specified by the PDEs, which are then transformed into nonlinear ODEs, take these presumptions into account.

2 Mathematical Modelling

In the present study, the nanofluid is treated as a single-phase effective fluid, and its thermophysical characteristics are represented through the corresponding effective fluid properties appearing in the governing equations. The present formulation focuses on the effects of magnetic field, thermal radiation, viscous dissipation, temperature-dependent heat source, concentration-dependent heat source, and chemical reaction. A laminar nanofluid flow over a stretching sheet subjected to Thompson and Troian slip conditions. An externally applied magnetic field is directed against the fluid motion, and viscous dissipation is included in the energy equation. The existence of nanoparticles within the nanofluid leads to chemical reactions which are modelled in the concentration equation. Furthermore, two heat sources are considered; temperature and concentration dependent. The physical configuration in the Cartesian plane with x-axis being the horizontal axis and y-axis is perpendicular as shown in Figure 1. With the above considerations, the mathematical model takes the following form of Eqs. (1)-(4)

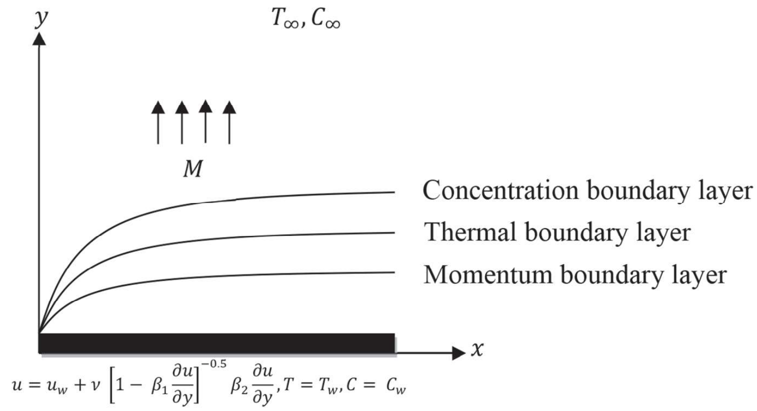

Figure 1 Physical Configuration

$$\frac{\partial u}{\partial x} + \frac{\partial v}{\partial y} = 0 \tag{1}$$

$$u\frac{\partial u}{\partial x} + v\frac{\partial u}{\partial y} = \nu\frac{\partial^2 u}{\partial y^2} - \frac{\sigma B_0^2}{\rho}u \tag{2}$$

$$u\frac{\partial T}{\partial x} + v\frac{\partial T}{\partial y} = \alpha\frac{\partial^2 T}{\partial y^2} + \frac{\overline{Q}_T}{\rho C_p}(T - T_w) + \frac{\overline{Q}_C}{\rho C_p}(C - C_w) + \frac{\mu}{\rho C_p}\left(\frac{\partial u}{\partial y}\right)^2 - \frac{1}{\rho Cp}\frac{\partial q_r}{\partial y} = 0 \tag{3}$$

$$u\frac{\partial C}{\partial x} + v\frac{\partial C}{\partial y} = D_B\frac{\partial^2 C}{\partial y^2} - K_r(C - C_w) \tag{4}$$

The flow is subjected to the following constraints:

$$u = u_w + \nu\left[1 - \beta_1\frac{\partial u}{\partial y}\right]^{-0.5}\beta_2\frac{\partial u}{\partial y},\ v = 0,\ T = T_w,\ C = C_w \text{ at } y = 0 \tag{5}$$

$$u \to 0,\ T \to T_\infty,\ C \to C_\infty \text{ as } y \to \infty$$

In the energy equation the Rosseland approximation is used to model the radiation term according to which the radiative heat flux q_r is defined as $\frac{4\sigma^*}{3k^*}\frac{\partial T^4}{\partial y}$. Assuming a small temperature difference within the layers of fluid, the T^4 term is expanded using Taylor series expansion about T_∞. This yields $T^4 = 4T_\infty^3 T - 3T_\infty^4$. Substituting this in the energy equation (3) simplifies it to

$$u\frac{\partial T}{\partial x} + v\frac{\partial T}{\partial y} = \alpha\left(1 + \frac{16T_\infty^3\sigma^*}{3k^*\kappa}\right)\frac{\partial^2 T}{\partial y^2} + \frac{\overline{Q}_T}{\rho C_p}(T - T_w) + \frac{\overline{Q}_C}{\rho C_p}(C - C_w) + \frac{\mu}{\rho C_p}\left(\frac{\partial u}{\partial y}\right)^2 = 0 \tag{6}$$

The similarity transformations that convert the system of PDEs to a system of nonlinear ODEs are as follows:

$$u = axf'(\eta),\ v = -\sqrt{a\nu}f(\eta),\ \theta(\eta) = \frac{T - T_\infty}{T_w - T_\infty},\ \phi(\eta) = \frac{C - C_w}{C_w - C_\infty},\ \eta = \sqrt{\frac{a}{\nu}}y$$

The quantities of physical parameters that act are defined as follows:

- Skin friction coefficient: $Cf_x = \frac{\mu}{\rho u_w^2}\left(\frac{\partial u}{\partial y}\right)_{y=0}$
- Nusselt number: $Nu_x = \frac{x}{\kappa(T_w - T_\infty)}\left[\kappa\left(\frac{\partial T}{\partial y}\right)_{y=0} - \frac{4\sigma^*}{3k^*}\left(\frac{\partial T^4}{\partial y}\right)_{y=0}\right]$
- Sherwood number: $Sh_x = -\frac{x}{D_B(C_w - C_\infty)}\left(\frac{\partial C}{\partial y}\right)_{y=0}$

The continuity equation (1) is satisfied for the above-defined similarity transformation and the resulting system of transformed equations are:

$$f''' + ff'' - f'^2 - Mf' = 0 \tag{7}$$

$$\left(1 + \frac{4}{3}R\right)\theta'' + Pr(Q_T\theta + Q_C\phi + f\theta') + Ecf''^2 = 0 \tag{8}$$

$$\phi'' + Scf\phi' - ScK\phi = 0 \tag{9}$$

Associated boundary conditions take the following form:

$$\begin{aligned} &f'(0) = 1 + \gamma\left[\frac{f''(0)}{\sqrt{1-\zeta f''(0)}}\right], \quad f(0) = 0, \quad \theta(0) = 1, \quad \phi(0) = 1, \quad \text{at} \quad \eta = 0 \\ &f'(\infty) \to 0, \quad \theta(\infty) \to 0, \quad \phi(\infty) \to 0, \quad \text{as} \quad \eta \to \infty \end{aligned} \tag{10}$$

The transformed form of the physical quantities are:

$$\sqrt{Re_x}Cf_x = f''(0), \frac{Nu_x}{\sqrt{Re_x}} = -\theta'(0), \frac{Sh_x}{\sqrt{Re_x}} = -\phi'(0) \tag{11}$$

The dimensionless fluid flow parameters appearing in this study are

$$M = \frac{\sigma B_0^2}{\rho a}, \alpha = \frac{\kappa}{\rho Cp}, R = \frac{4\sigma^* T_\infty^3}{3k^*\kappa}, Sc = \frac{\nu}{D_B}, Pr = \frac{\nu}{\alpha}, \overline{Q}_T = \frac{Q_T}{a(\rho Cp)},$$

$$\overline{Q}_C = \frac{Q_C}{a(\rho Cp)}\left(\frac{C_w - C_\infty}{T_w - T_\infty}\right), Ec = \frac{\mu}{\rho Cp}\left(\frac{a^2x^2}{\alpha(T_w - T_\infty)}\right)$$

Nomenclature

Greek		C	Concentration
α	Thermal diffusivity	C_w	Concentration at the wall
β_1	Navier's invariable slip	C_∞	Ambient concentration
β_2	Inverse of critical shear rate	T	Temperature
γ	Slip parameter	T_w	Temperature at the wall
κ	Thermal conductivity	T_∞	Ambient temperature
μ	Dynamic viscosity	Sh_x	Sherwood number
ν	Kinematic viscosity	Nu_x	Nusselt number
ρ	Density	Re_x	Reynolds number
σ	Electrical conductivity	Cf_x	Skin friction coefficient
$\sigma*$	Stefan – Boltzmann constant	R	Radiation parameter
ζ	Dimensionless critical shear rate	D_T	Thermophoresis diffusivity

	Roman	D_B	Brownian motion diffusivity
$k*$	Mean absorption coefficient	K	Chemical reaction parameter
a	Time inverse constant	K_r	Chemical reaction
B_0	Magnetic field	M	Magnetic field parameter
u, v	Velocity components	Pr	Prandtl number
x, y	Coordinates	Sc	Schmidt number
u_w	Stretching sheet velocity	q_r	Thermal radiation
$\bar{Q}_T$	Temperature dependent heat source	Q_C	Dimensionless concentration dependent heat source
Ec	Eckert number	Q_T	Dimensionless temperature dependent heat source
$\bar{Q}_C$	Concentration dependent heat source		

3 Solution Methodology

The first order ODEs are solved using a numerical strategy called Runge Kutta Fehlberg (RKF-45) method. This method produces an accurate and efficient solution and incorporates Runge Kutta methods of fourth and fifth order. Adaptive step size control is made possible where the step size is dynamically changed based on the approximated error between the fourth and fifth order solutions. This approach solves a wide range of problems accurately and efficiently, making it highly useful when extreme precision is needed. Since it automatically controls the error and optimizes processing effort, it is a widely used method in scientific and technical computing. The precision level is set at 10^(-6). The system of equations (7)-(10) are reformulated into a system of first-order differential equations which are then solved using this technique. The obtained solutions are thus compared with the existing literature and an acceptable accuracy is recorded as shown in Table 1.

Table 1: Validation of results

M	$\sqrt{Re_x}\,Cf_x$		
	Khan et al. [25]	Mukhopadyay [26]	Present
0	1.00000	1.00000	1.00000
0.25	−1.11803	−1.11803	−1.11803
1	−1.41421	−1.41213	−1.41421
2.25	−1.80278	−1.80277	−1.80278

4 Results and Discussion

Figure 2 depicts the influence of magnetic field parameter, M on velocity profile. As M increases, velocity profile reduces. The Lorentz force induces the velocity distribution to decline as the magnetic field parameter exhibits an increment. This force produces a drag-like effect by acting opposite to the fluid velocity. The drag reduces the momentum and velocity of the fluid. Figure 3 illustrates how slip parameter, γ effects on velocity profile. With higher slip parameter, the reduced adhesion between the fluid and the solid results in a fall in the velocity profile because the fluid can move more freely and the shear stress at the wall is reduced. Figure 4 represents how thermal radiation, R, have an impact on the thermal profile.

As R increases, the thermal profile increases. An object's temperature shows an upward trend in response to an increase in thermal radiation because of an increase in energy absorption. By raising its temperature, the object's thermal profile is modified, affecting how heat is distributed.

Figure 5 shows that the temperature-dependent heat source, Q_T, increases the temperature profile. The process can become self-reinforcing, raising the temperature profile even further when the heat source intensifies because the heat source is temperature-dependent. The effect of temperature profile, Q_C, and concentration-dependent heat source are depicted in Figure 6. As Q_C increases, thermal profile also increases. Temperature also rises due to increased heat generation within the material when a concentration-dependent heat source increases. This extra heat source alters the temperature distribution.

Figure 7 represents the influence of Schmidt number, S_C, on the concentration profile. The concentration profile is seen to reduce as Sc increases. A higher ratio of mass diffusivity to momentum diffusivity is indicated by an increasing Schmidt number indicating that the fluid is more capable at spreading momentum than mass. A greater rate of change in concentration and a more constrained concentration profile makes mass diffusion less effective. Figure 8 illustrates that increasing the chemical reaction rate K, causes a reduction in the concentration profile. Reactants are consumed which causes their concentration to drop more quickly over time. As a result, the concentration profile becomes greater and the reactant concentration falls off quickly. This effect is more noticeable at higher reaction rates because reactants are transformed into products more quickly, which decreases their availability in the system.

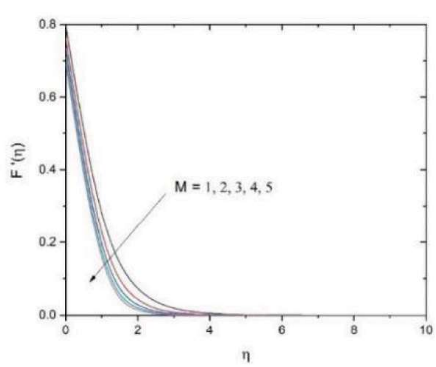

Figure 2: Variations of $F'(\eta)$ for M

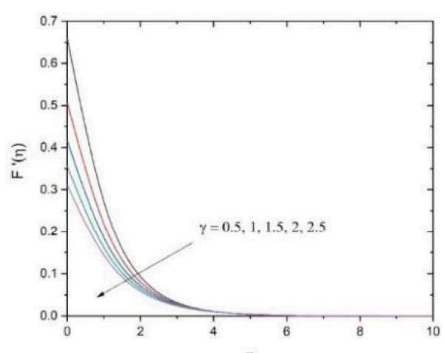

Figure 3: Variations of $F'(\eta)$ for γ

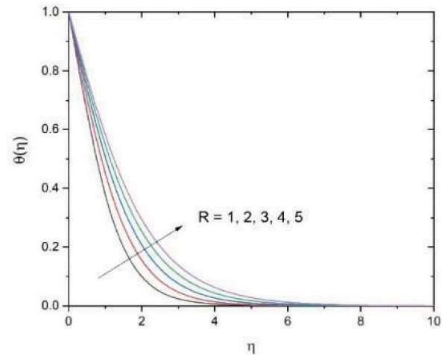

Figure 4: Variations of θ (η) for R

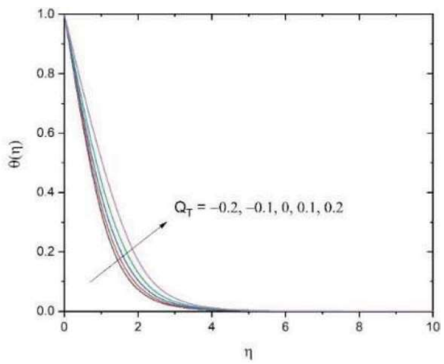

Figure 5: Variations of θ (η) for Q_T

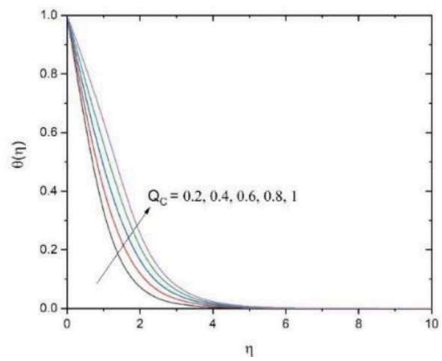

Figure 6: Variations of θ (η) for Q_C

Figure 9 represents the effect of skin friction coefficient, $Cf_x\sqrt{Re_x}$ for M and R. Owing to the mixed influence of thermal radiation and the magnetic field parameter, the skin friction coefficient rises. Higher thermal radiation raises the temperature and viscosity of the fluid, whereas the Lorentz force adds resistance as the magnetic field value increases. The combined effect of these factors raises the boundary's shear stress, which raises the skin friction coefficient. Figure 10 shows the influence of M and R on Nusselt number. Because of the Lorentz effect, the Nusselt number drops as M increases. This force acts against the direction of the fluid flow, impeding its mobility resulting in diminished heat transfer. A drop in the Nusselt number might result from an increase in heat radiation. This is due to the fact that higher thermal radiation can raise the temperature of the fluid, which can result in a thicker thermal boundary layer and less effective heat transmission.

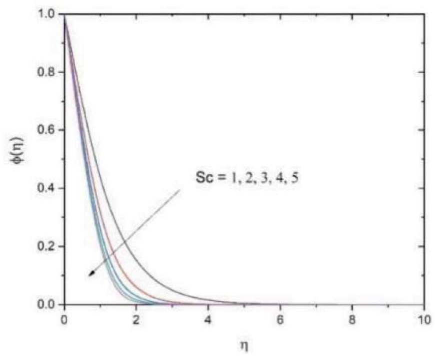

Figure 7: Variations of ϕ (η) for S_C

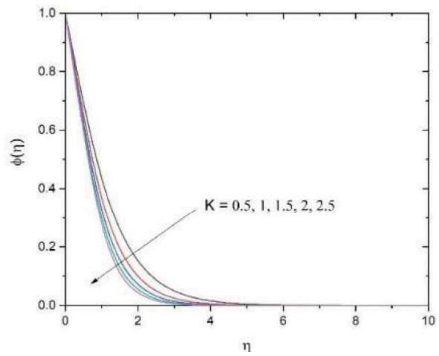

Figure 8: Variations of ϕ (η) for K

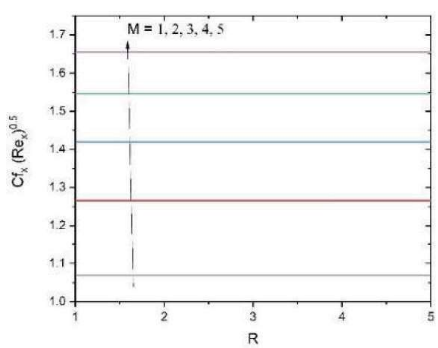

Figure 9: Variations of $Cf_x\sqrt{Re_x}$ for $M\, and\, R$

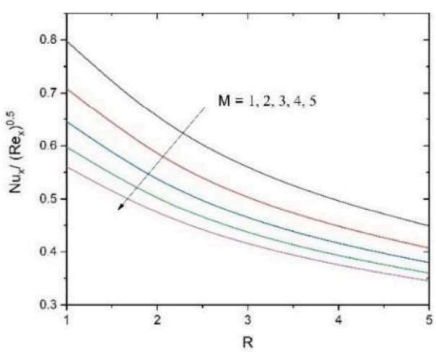

Figure 10: Variations of $\frac{Nu_x}{\sqrt{Re_x}}$ for $M\, and\, R$

Figure 11 represents the effect on Sherwood number for *M* and *R*. Sherwood number decreases for various values of *M* and *R*. The fluid's velocity is opposed by a Lorentz force created by a magnetic field. Because of this resistance, there is less convective mass transfer, which lowers the Sherwood number. Furthermore, thermal radiation makes the fluid's energy more accessible, which may improve its mass diffusivity but may also decrease its thermal conductivity. Lowering the Sherwood number can also be contributed to this decrease in mass diffusivity. Figure 12 shows the effect on Nusselt number for *Sc* and *K*. Nusselt number increases with *Sc* and *K*. A faster rate of chemical reaction within the fluid might result in more heat being generated, which raises the temperature gradient and promotes convective heat transfer. Higher mass diffusivity, which might facilitate the movement of species that carry heat and hence raise the Nusselt number, is also indicated by a lower Schmidt number.

Figure 13 shows the effect on Sherwood number, for *Sc* and *K*. Higher values of *Sc* and *K* result in an enhanced Sherwood number. A lower mass diffusivity, which may increase the concentration disparity and promote convective mass transfer, is indicated by a larger Schmidt number. Furthermore, a faster rate of chemical reaction may result in the diffusing species being consumed more quickly, which would raise the concentration gradient and raise the Sherwood number. Figure 14 indicates how the Nusselt number, $\frac{Nu_x}{\sqrt{Re_x}}$ changes for different values of Q_T and Q_C. N decreases for different values of Q_T and Q_C . By decreasing the temperature gradient and promoting convective heat transmission, a temperature dependent heat source might lead to enhanced uniform temperature distribution throughout the fluid. Heat transfer can also be impacted by a concentration-dependent heat source, which can produce a more uniform concentration profile by lowering the concentration gradient and restricting convective mass transfer.

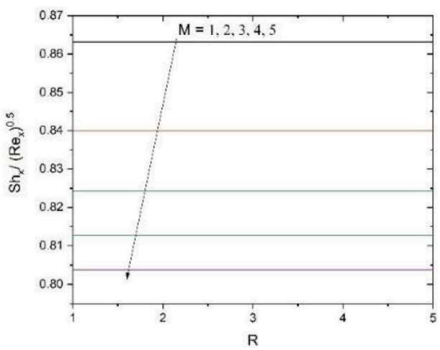

Figure 11: Variations of $\frac{Sh_x}{\sqrt{Re_x}}$ for $M \, and \, R$

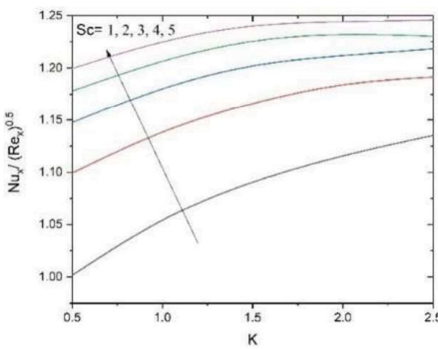

Figure 12: Variations of $\frac{Nu_x}{\sqrt{Re_x}}$ for $Sc \, and \, K$

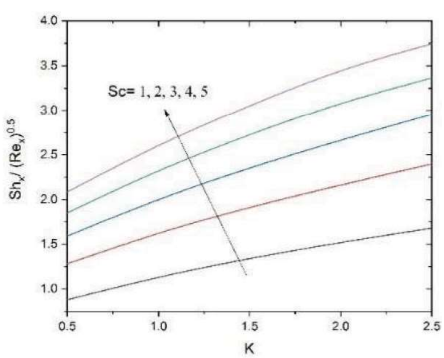

Figure 13: Variations of $\frac{Sh_x}{\sqrt{Re_x}}$ for $Sc \, and \, K$

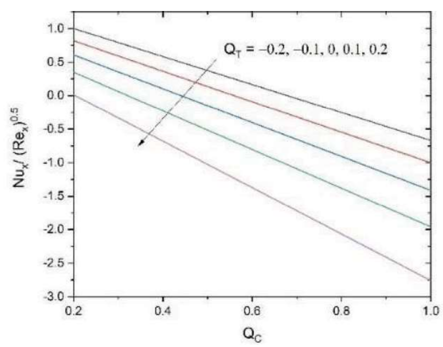

Figure 14: Variations of $\frac{Nu_x}{\sqrt{Re_x}}$ for $Q_T \, and \, Q_C$

5 Conclusion

The flow dynamics of a nanofluid over a stretching sheet are analysed with Thompson and Troian slip boundary conditions. The energy equation was modelled by integrating the viscous dissipation effect, and concentration-dependent and temperature-dependent heat sources. Whereas, the concentration equation was modelled by considering the effect of chemical reaction. All these assumptions were inserted into differential equations and with the help of RKF-45 method, the solutions were obtained. The results were interpreted in the form of graphs and the major outcomes are follows:

- The rise in the externally applied magnetic field diminished the movement of the nanofluid velocity establishing its assistance in effective control of the flow.
- The higher values of K, reduced the concentration as the nanoparticle's interaction led to the chemical reactions the resulted in chemically stable particles.
- Both, concentration dependent and temperature dependent heat sources enhanced the temperature profile of the nanofluid.
- The Schmidt number enhanced the diffusivity and lead to the decrease in the concentration profile.

References

[1] Patel, S., and Patel, H. R. "Magnetohydrodynamics bio-convection flow at Casson fluid stagnation point in porous medium: Cross-diffusion effect and heat production." *Propulsion and Power Research* (2024).

[2] Jamrus, F. N., Waini, I., and Ishak, A. "Time-Depending Flow of Ternary Hybrid Nanofluid Past a Stretching Sheet with Suction and Magnetohydrodynamic (MHD) Effects." *Journal of Advanced Research in Fluid Mechanics and Thermal Sciences* 117 (2024): 15-27.

[3] Hajool, S. S., and Harfash, A. J. "Magnetohydrodynamic instability of fluid flow in a bidisperse porous medium." *Journal of Engineering Mathematics* 147 (2024): 10.

[4] Waini, I., Ishak, A., and Pop, I. "Eyring-Powell Fluid Flow Past a Shrinking Sheet: Effect of Magnetohydrodynamic (MHD) and Joule Heating." *Journal of Advanced Research in Fluid Mechanics and Thermal Sciences* 116 (2024): 64-77.

[5] Fard, M. S., Torabiyan, A., Jalili, B., and Ganji, D. D. "Investigating the magnetohydrodynamics non-Newtonian fluid movement on a tensile plate affected by variable thickness with dufour and soret effects: Akbari Ganji and finite element methods." *International Journal of Electrochemical Science* 19 (2024): 100701.

[6] Rehman, A., and Khan, I. "Mixed convection flow of hybrid nanofluids with viscous dissipation and dynamic viscosity." *BioNanoScience* 14 (2024): 946-954.

[7] Rehman, A., Khan, D., Mahariq, I., Elkotb, M. A., and Elnaqeeb, T. "Viscous dissipation effects on time-dependent MHD Casson nanofluid over stretching surface: A hybrid nanofluid study." *Journal of Molecular Liquids* 408 (2024): 125370.

[8] Ul Haq, S., and Ashraf, M. B. "Non-similar solution of mixed convection flow of viscous fluid over curved stretching surface with viscous dissipation and entropy generation." *Numerical Heat Transfer, Part B: Fundamentals* 85 (2024): 177-198.

[9] Awais, M., Salahuddin, T., and Muhammad, S. "Effects of viscous dissipation and activation energy for the MHD Eyring-powell fluid flow with Darcy-Forchheimer and variable fluid properties." *Ain Shams Engineering Journal* 15 (2024): 102422.

[10] Maaitah, H., Obalid, A. M., Abel, M. S., and Al-Sarayreh, A. "Viscous dissipation analysis of Williamson fluid over a horizontal saturated porous plate at constant wall temperature." *International Journal of Thermofluids* 19 (2023): 100361.

[11] Zhang, J., Qi, N., and Jiang, J. "Effect of oil viscosity on hydraulic cavitation luminescence." *Fluid Dynamics* 56 (2021): 371-382.

[12] Rudyak, V. Ya. "Specific features of modeling nanofluid flows (a review)." *Fluid Dynamics* 59 (2024): 1072-1087.

[13] Nuriev, A. N., Zainuganov, A. M., Shishkin, O. N., and Egorov, A. G. "Asymptotic study of flows induced by oscillations of cylindrical bodies." *Fluid Dynamics* 59 (2024): 314-330.

[14] Majeed, A. H., Mahmood, R., Shahzad, H., and Awan, M. B. "Heat and mass transfer characteristics in MHD Casson fluid flow over a cylinder in a wavy channel: Higher-order FEM computations." *Case Studies in Thermal Engineering* 42 (2023): 102730.

[15] Abbas, S., Awan, M. B., Raza, A., Malik, M. Y., and Albalawi, A. M. "Heat and mass transfer through a vertical channel for the Brinkman fluid using Prabhakar fractional derivative." *Applied Thermal Engineering* 232 (2023): 121065.

[16] Ahmad, S., Cham, B. M., Liu, D., and Khan, S. U. "Numerical analysis of heat and mass transfer of MHD natural convection flow in a cavity with effects of source and sink." *Case Studies in Thermal Engineering* 53 (2024): 103926.

[17] Karim, M. F., Munshi, M. J. H., Rahman, M. M., Uddin, M. J., and Alim, A. I. "A numerical investigation on forced convection heat and mass transfer performance in a right triangular cavity." *International Journal of Thermofluids* 21 (2024): 100578.

[18] Kumar, V. V., Shekar, M. N. R., and Bejawada, S. G. "Heat and Mass Transfer Significance on MHD Flow over a Vertical Porous Plate in the Presence of Chemical Reaction and Heat Generation." *CFD Letters* 16 (2024): 9-20.

[19] Menni, Y., Chamkha, A. J., Ahmed, C. S. B. B. H. M., and Ameur, H. "Enhancing heat transfer performance: A comprehensive review of perforated obstacles." *Fluid Dynamics* 71 (2025): 1-21.

[20] Thompson, P. A., and Troian, S. M. "A general boundary condition for liquid flow at solid surfaces." *Nature* 389 (1997): 360-362.

[21] Xin, X., Zhang, X., Zhang, Y., and Dong, Z. "The flow analysis of Williamson nanofluid considering the Thompson and Troian slip conditions at the boundary." *Numerical Heat Transfer, Part A: Applications* 85 (2024): 1937-1953.

[22] Shaheen, N., Mushtaq, A., Zafar, S., and Ramzan, M. "Analysis of Newtonian heating and surface catalyzed reaction in a trihybrid nanofluid flow across an expanding/shrinking cylinder with Thompson and Troian slip." *Proceedings of the Institution of Mechanical Engineers, Part N: Journal of Nanomaterials, Nanoengineering and Nanosystems* (2024): 23977914231225174.

[23] Mishra, A. "Thompson and Troian slip effects on ternary hybrid nanofluid flow over a permeable plate with chemical reaction." *Numerical Heat Transfer, Part B: Fundamentals* (2024): 1-29.

[24] Chaudhary, S., and Deshwal, J. "Thompson and Troian velocity slip flow of the Casson hybrid nanofluid past a Darcy–Forchheimer porous inclined surface with Ohmic heating, Dufour and Soret effects." *Pramana* 98 (2024): 55.

[25] Khan, U., Zaib, A., Alharbi, A. M., Abed, A. M., and Khan, I. "Features of hybridized AA7072 and AA7075 alloys nanomaterials with melting heat transfer past a movable cylinder with Thompson and Troian slip effect." *Arabian Journal of Chemistry* 16 (2023): 104503.

[26] Mukhopadhyay, S. "MHD boundary layer slip flow along a stretching cylinder." *Ain Shams Engineering Journal* 4 (2013): 317-324.